Article

Dynamics of Changes in Climate Zones and Building Energy Demand. A Case Study in Spain

Carmen Díaz-López [1], Joaquín Jódar [2], Konstantin Verichev [3], Miguel Luis Rodríguez [4], Manuel Carpio [5] and Montserrat Zamorano [1,*]

[1] Department of Civil Engineering, ETS Ingenieria de Caminos, Canales y Puertos, Campus Fuentenueva s/n, University of Granada, 18071 Granada, Spain; carmendiaz@ugr.es
[2] Department of Mathematics, Campus Las Lagunillas, University of Jaén, 23071 Jaén, Spain; jjodar@ujaen.es
[3] Institute of Civil Engineering, Universidad Austral de Chile, General Lagos 2050, Valdivia 5111187, Chile; konstantin.verichev@uach.cl
[4] Department of Applied Mathematics, Campus Fuentenueva, University of Granada, 18071 Granada, Spain; miguelrg@ugr.es
[5] Department of Construction Engineering and Management, School of Engineering, Pontificia Universidad Católica de Chile, Avenida Vicuña Mackenna 4860, Santiago 7820436, Chile; manuel.carpio@ing.puc.cl
* Correspondence: zamorano@ugr.es; Tel.: +34-958-249-458

Abstract: In the current context of the climate crisis, it is essential to design buildings that can cope with climate dynamics throughout their life cycle. It will ensure the development of sustainable and resilient building stock. Thus, this study's primary objective has been to demonstrate that the current climatic zones for buildings in peninsular Spain do not represent the current climatic reality and are not adapted to climate change and the impact on the energy demand of buildings. For this reason, the climatic zones of 7967 peninsular cities have been updated and adapted to the RCP 4.5 and RCP 8.5 scenarios by using the data measured in 77 meteorological reference stations. The results obtained have shown that in more than 80% of the cities, buildings are designed and constructed according to an obsolete climatic classification that does not take into account the current or future climatic reality, which will significantly affect the thermal performance of a building and highlights the need to review the climatic zoning in the country. The results obtained can be extrapolated to other regions. The methodology defined in this work can be used as a reference, thus making an essential scientific contribution in reflecting on current capacities and the possibilities of improving the building stock.

Keywords: climate zone; climate change; building; energy demand; building resilience

1. Introduction

According to the fifth assessment report of the Intergovernmental Panel on Climate Change (IPCC), compared to values from 1850 to 1900, the global land surface temperature increased by 0.85 °C between 1880–2012 and 0.78 °C between 2003–2012 [1]. Projections of future climate conditions [1], predict an increase in global average temperature by the year 2100 in the range 1.4 to 5.8 °C [2], revealing an increasing disparity between historical climate patterns and current and future climate conditions resulting from anthropogenic changes [3].

This report also presents a set of four possible scenarios of climate change, called Representative Concentration Pathways (RCPs) [4]. These scenarios are characterized by the approximate calculation that gives the Radiative Forcing (RF) in the year 2100, with respect to the year 1750, taking into consideration different trajectories for emissions of long-lived greenhouse gases (LLGHGs) and short-lived air pollutants, the corresponding concentration levels and land use [3]. In the following, a description is given of the two scenarios within which the present study is realized. These scenarios were selected due to their wide application in other studies related to climate change, building EC, and climate zones for buildings [4].

RCP 4.5. An intermediate stabilization pathway in which RF is stabilized at approximately 4.5 W/m^2 after 2100. It will be necessary to limit emissions through increased use of electricity, lower-emission energies, CO_2 capture technologies, and geological storage. The area of forests is also expected to increase for this scenario, compared to the current state. Furthermore, CO_2 emissions from energy and industrial sources are expected to increase until 2040 and then decrease to the prescribed atmospheric CO_2 concentration of 538 ppm in 2100. At the same time, by 2081–2100, the global mean surface temperature will increase by 1.8 °C (likely range 1.1 to 2.6 °C) compared to the 1986–2005 climate period [5,6].

RCP 8.5. During the 21st century, RF will grow steadily and reach 8.5 W/m^2 in 2100. Very high GHG emissions characterize the scenario. RCP 8.5 combines the assumptions of a steady increase in the global population, a moderate rate of technological change, and energy intensity improvements. In the long term, this leads to high energy demand and GHG emissions in the absence of a climate change policy. The prescribed CO_2 concentration is 936 ppm in 2100. At the same time, by 2081–2100, the global mean surface temperature will increase by 3.7 °C (likely range 2.6 to 4.8 °C) compared to 1986–2005 [7,8].

Consequently, in the future, the temperature increase will determine the setting of new energy budgets; indeed, climate change is transforming buildings and cities' energy performance [8,9]. Thus, numerous studies show that it is essential to take climate dynamism into account in the building design phase; otherwise, the estimated energy demand (ED) could triple [9–12]. For example, Christenson et al. 2006 [13], showed how global warming's impact increases the cooling energy demand of buildings. In the study by de Rosa et al. 2014 [14], a simplified building dynamic model, based on the electrical analogy, was developed and implemented in a Matlab/Simulink environment in order to perform several analyses on heating (H) and cooling (C) energy demand in a wide range of climatic conditions. Verichev et al. 2020 [6] showed the effects of climate change on variations in climatic zones and heating energy consumption of residential buildings in southern Chile under different climate change scenarios. Thus, in the general context of global warming, in cold regions, the intensity of energy consumption reduction will be greater than the intensity of increase in cooling energy consumption [15,16]. Similarly, numerous studies conclude that in regions with a warm climate, the heating energy consumption (EC) of buildings will decrease. At the same time, the cooling EC will increase in conjunction with an increase in days of indoor thermal discomfort [17–25].

Currently, there are not many studies to assess the evolution of climatic zones for buildings. For example, in the study of Zhai and Helman 2019, the authors use data from 23 climate models, but the evolution of building climates is analyzed in only seven cities in the United States [26]. In China, the evolution of ASHRAE building climatic zones was analyzed based on data from 5 climate models for the RCP 4.5 scenario [27]. In the case of the analysis of the climatic zones of ASHRAE, it is quite convenient to use the data of climatic models on the daily maximum and minimum temperatures for future periods without additional modifications. On the other hand, some studies use the morphing methodologies described in the study of Belcher et al. 2005 [28]. For example, in the study of the dynamics of climatic zones for construction in Chile [6]; in study of risk of overheating increases of residential buildings in Sweden [29]; evaluation of life cycle impacts of buildings, integrating climate change effect and evolution of the energy mix in the long term in France [30].

At the same time, to assess thermal comfort or to simulate building energy consumption in future climatic conditions, it is necessary to use more complex methodologies for morphing meteorological data, taking into account changes in the intraday variability of meteorological parameters [31,32]. Additionally, in some studies, special tools are used to generate meteorological files for future periods, such as OZClim [33] or CCWorldWeatherGen [34].

In order to mitigate and adapt to these climate effects, the European Commission presented Directive (EU) 2018/844 [35] of the European Parliament and the Council of 30 May 2018 on energy efficiency, which, together with the European Green Deal [36], will adopt a new and more ambitious EU strategy on adaptation to climate change. In this context, many countries have developed regulations based on climate zone classification, a beneficial method to design buildings with lower energy consumption [37–39], and high thermal comfort [40]. This method is based on analyzing large amounts of meteorological, environmental, and social data to contribute to the search for climate models that absorb all of the above [41]. The number of climate zones depends on each country, the thresholds set, and the methodology used. For example, Spain, in the Technical Building Code (CTE in Spanish) [42], establishes 15 climate zones (α3, A2, A3, A4, B2, B3, B4, C1, C2, C3, C4, D1, D2, D3, E1) identified by a letter corresponding to the climatic severity in winter (α, A, B, C, D, and E) and a number (1, 2, 3, and 4) corresponding to the summer values. Portugal establishes nine climate zones (I1-V1, I1-V2, I1-V3, I2-V1, I2-V2, I2-V3, I3-V1, I3-V2, I3-V3) from the different combinations of winter letters (V1, V2, and V3) and summer letters (I1, I2, and I3) [43]; France establishes eight zones (H1a, H1b, H1c, H2a, H2b, H2c, H2d, H3), taking into account winter temperatures (H1, H2, and H3) and summer temperatures (a, b, c, and d) [44]. In any case, the climatic zonings used in different countries are based on the climatic series existing at the time of their formulation, and therefore do not allow the design of building parks capable of adapting to climatic dynamism [45].

Consequently, it is essential to design and construct buildings capable of assuming the climatic dynamics throughout their life cycle. Knowledge of the climatic reality will guarantee the development of a building stock that is certainly sustainable and resilient. For this reason, the main objective of this work has been to analyze the dynamics of changes in climate zones and their effect on the energy demand of buildings. Spain has been selected as the study area due to its climatic variety, which will allow the applied methodology, results, and conclusions obtained to be used as a reference in other regions. Furthermore, in this country, there is low investment in sustainable building, with the construction sector being one of its primary energy consumers, which translates into one of the highest consumption rates per Gross Domestic Product (GDP) in the European Union [46], highlighting the urgent need to take measures to solve this problem.

2. Materials and Methods

An update of the CTE climate zones [42] of 7967 localities of peninsular Spain has been carried out, under two of the four scenarios called Representative Concentration Pathways (RCPs) (RCP 2.6, RCP 4.5, RCP 6.0, and RCP 8.5), specifically RCP 4.5 and RCP 8.5 scenarios, to achieve the objective of this study. These scenarios are characterized by their approximate calculation of the total RF in the year 2100, relative to 1750 [6]. Each scenario describes a different trajectory for long-lived greenhouse gas emissions (LLGHGs) and short-lived air pollutants, the corresponding concentration levels, land use, and radiative forcing [5]. Besides, to know the effect of this dynamic of changes in buildings' energy consumption, a typical dwelling has been taken as a reference, and the evolution of its energy demand has been analyzed. The description of the bases for the definition of CTE climate zones and the methodology applied for this purpose is described below.

2.1. Basis for the Definition of CTE Climate Zones

In Spain, the CTE and its Basic Document on Energy Saving (DB-HE) [42] establishes a methodology that allows the definition of climatic zones for buildings. This methodology is based on the concept of climatic severity index (CSI), a unique number on a dimensionless scale that is specific for each geographical location [47] and that allows differentiating between climatic severity index for summer (SCS) and winter (WCS).

The WCS and SCS indices are obtained by applying Equations (1) and (2) [42], respectively, where $HDD20_{oct-may}$ is the sum of winter degree-days in 20 °C bases for the months ranging from October to May, calculated through the hourly method; $CDD20_{jun-sep}$ is the sum of summer degree-days in 20 °C bases for the months ranging from June to September, calculated through the hourly method; a, b, c, d, and e are the regression coefficients whose values are $a = 3.546 \times 10^{-4}$, $b = -4.043 \times 10^{-1}$, $c = 8.394 \times 10^{-8}$, $d = -7.325 \times 10^{-2}$, $e = -1.137 \times 10^{-1}$, in the case of WCS, and $a = 2.990 \times 10^{-3}$, $b = -1.1597 \times 10^{-7}$, $c = -1.713 \times 10^{-1}$, in the case of SCS; n is the sum of sunshine duration hours in the period from October to May; and N is the sum of the maximum possible of sunshine duration hours for the months from October to May.

$$WCS = a \cdot HDD20_{oct-may} + b \cdot \frac{n}{N} + c \cdot HDD20_{oct-may}^2 + d \cdot \left(\frac{n}{N}\right)^2 + e \tag{1}$$

$$SCS = a \cdot CDD20_{jun-sep} + b \cdot CDD20_{jun-sep}^2 + c \tag{2}$$

Each of the six winter climate zones defined in the DB-HE is assigned a letter (α, A, B, C, D, and E) corresponding to the WCS interval indicated in Table 1, with the climate zone α having the warmest winter and E the coldest [16]. By the four summer climate zones defined in the DB-HE and identified with a number (1, 2, 3, and 4), these are determined according to the SCS. Besides, it corresponds to the interval indicated in Table 1, being one the climate zone with the least warm summer and four the warmest [42]. Finally, the combination of letter and number given in Table 1 is the one that generates the building climate zone code for any city or geographical location. According to the provisions of the DB-HE document of CTE in peninsular Spain, there are 12 possible combinations and, as a result, climate zones (A3, A4, B3, B4, C1, C2, C3, C4, D1, D2, D3, and E1).

Table 1. Intervals for climate zoning.

Intervals for Winter Zoning					
α	A	B	C	D	E
$WCS \leq 0$	$0 < WCS \leq 0.23$	$0.23 < WCS \leq 0.5$	$0.5 < WCS \leq 0.93$	$0.93 < WCS \leq 1.51$	$WCS > 1.51$
Intervals for Summer Zoning					
1	2	3	4		
$SCS \leq 0.5$	$0.5 < SCS \leq 0.83$	$0.83 < SCS \leq 1.38$	$SCS > 1.38$		

2.2. Methodology

The methodology used to achieve the objectives of this work consists of four phases, which are described in the following sections:

(i)   Determination of climate severity indices.
(ii)   Determination of the dynamics of changes in climate severity indices.
(iii)   Proposal for updating climate zones for peninsular Spain.
(iv)   Evaluation of the dynamics of changes in energy demand in housing.

2.2.1. Determination of Climate Severity Indices

From among the almost 800 weather stations located by the State Meteorological Agency (AEMET) in peninsular Spain [48], whose data can be provided for research, a total of 77 were selected (Figure 1 and Table 2). Considering their proximity to urban centers and a homogeneous distribution based on these centers' population, they were also sought with a minimum measurement period of 3 years, between 2015–2018, and which had hourly temperature measurement data available. As for the data relating to sunshine duration hours, 55 of them were able to provide them; in the case of the remaining 22 stations, the data from the geographically closest station that had them was used.
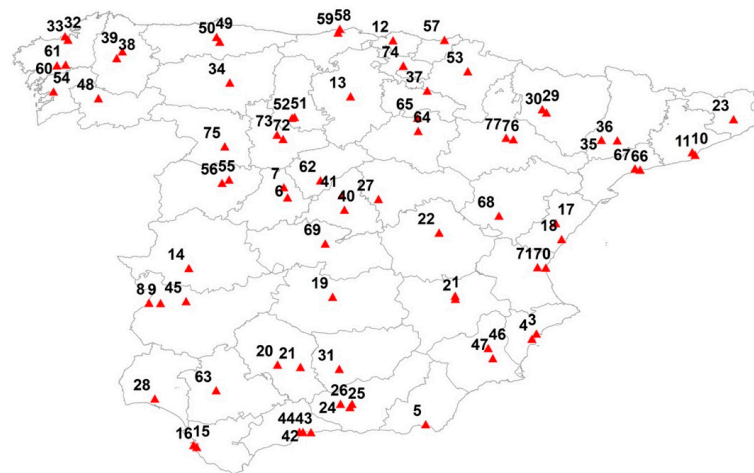
Figure 1. Geographical location of AEMET weather stations.

Table 2. Calculated indices of winter (WCS) and summer (SCS) climate severity for the period 2015–2018.

WS	Latitude	Longitude	Altitude	WCS	SCS	WS	Latitude	Longitude	Altitude	WCS	SCS
1	39.00556	−1.862222	676	0.94	1.64	40	40.45167	−3.724167	664	0.96	1.76
2	38.95417	−1.856389	702	0.92	1.53	41	40.69611	−3.765000	1004	1.11	1.19
3	38.37250	−0.494167	22	0.14	1.74	42	36.71667	−4.419722	25	−0.01	1.52
4	38.28278	−0.570833	43	0.23	1.82	43	36.71500	−4.286111	7	−0.06	1.91
5	36.84691	−2.356989	21	0.20	1.75	44	36.71778	−4.481667	54	0.04	1.90
6	40.65917	−4.680000	1130	1.44	0.88	45	38.91583	−6.385556	228	0.57	1.98
7	40.82889	−4.741944	920	1.36	1.04	46	38.12806	−1.305833	150	0.17	2.05
8	38.88750	−7.008056	175	0.56	2.08	47	37.95778	−1.228611	75	0.21	2.15
9	38.88333	−6.813889	185	0.49	2.08	48	42.32528	−7.859722	442	0.84	1.11
10	41.41833	2.124167	408	0.61	0.92	49	43.35333	−5.874167	336	0.90	0.12
11	41.37500	2.173889	5	0.23	1.48	50	43.27500	−5.819167	170	0.86	0.29
12	43.29806	−2.906389	42	0.74	0.43	51	42.00944	−4.560556	736	1.41	0.93
13	42.35694	−3.620278	891	1.61	0.57	52	41.99556	−4.602778	874	1.54	0.71
14	39.47139	−6.338889	10	0.62	2.04	53	42.77750	−1.649722	459	1.02	0.75
15	36.49972	−6.257778	2	−0.02	1.38	54	42.43833	−8.615833	108	0.69	0.43
16	36.46556	−6.205556	28	0.00	1.380	55	40.95750	−5.662222	775	1.15	1.12
17	40.22722	−0.169722	10	0.67	1.24	56	40.90361	−5.779722	817	1.45	1.00
18	39.95722	−0.071944	43	0.22	1.70	57	43.30639	−2.041111	251	0.82	0.09
19	38.98917	−3.920278	628	0.80	2.16	58	43.49111	−3.800556	52	0.57	0.04
20	37.84889	−4.846667	90	0.37	2.52	59	43.42861	−3.831389	3	0.65	0.30
21	37.81028	−4.462222	275	0.41	2.42	60	42.87611	−8.555833	240	0.83	0.37
22	40.06722	−2.131944	948	1.13	1.38	61	42.88806	−8.410556	370	0.97	0.32
23	41.97222	2.819444	76	0.69	1.45	62	40.94528	−4.126389	1005	1.28	1.04
24	37.18972	−3.789444	567	0.61	2.10	63	37.41667	−5.879167	34	0.16	2.420
25	37.13722	−3.631389	687	0.64	1.79	64	41.77500	−2.483056	1082	1.54	0.710
26	37.18972	−3.595556	775	0.60	1.89	65	41.99583	−2.494167	1260	1.87	0.360
27	40.63028	−3.150000	721	0.95	1.69	66	41.12389	1.249167	55	0.35	1.440
28	37.27833	−6.911667	19	0.17	1.74	67	41.14500	1.163611	71	0.44	1.270
29	42.13889	−0.395000	463	0.97	1.40	68	40.35056	−1.124167	900	1.28	1.090
30	42.08444	−0.325556	546	1.03	1.26	69	39.88472	−4.045278	515	0.74	2.200
31	37.77750	−3.808889	580	0.42	2.33	70	39.47972	−0.337500	6	0.22	1.430
32	43.36583	−8.421389	58	0.55	0.04	71	39.48500	−0.474722	56	0.34	1.650
33	43.30694	−8.371944	98	0.76	0.12	72	41.64083	−4.754444	735	1.27	1.120
34	42.58833	−5.651111	912	1.55	0.33	73	41.71194	−4.855556	846	1.51	0.760
35	41.62611	0.598056	185	0.89	1.63	74	42.87194	−2.732778	513	1.32	0.460
36	41.61694	0.866667	252	0.95	1.39	75	41.51556	−5.735278	656	1.18	1.260
37	42.45222	−2.331111	353	1.01	0.92	76	41.63333	−0.882222	258	0.34	1.580
38	42.99833	−7.552500	442	1.18	0.38	77	41.66056	−1.004167	249	0.72	1.550
39	43.11139	−7.457500	445	1.25	0.25						

At each of these stations, the WCS and SCS indices were calculated using as a basis for calculation Equations (1) and (2) of the CTE [42] described in the previous section. In the case of Equation (1), the values of N, for each geographical location of stations, were calculated with the application "NOAA solar calculations year" [49] by the NOAA Earth System Research Laboratory (ESRL) Global Monitoring Division.

2.2.2. Determining the Dynamics of Changes in Climate Severity Indices

The calculation of the changes for the WCS and SCS indices of each of the stations was carried out using the Climate Change Adaptation Platform (AdapteCCa) [50] which contains the results of daily minimum and maximum temperature projections for the RCP 4.5 and RCP 8.5 scenarios from a total of 16 climatological models.

Based on the projection data and current hourly temperature measurement data from AEMET, for each of the 77 meteorological stations, firstly, the difference values (or deltas) of the monthly average temperature between the baseline climate period (2018) and the two future periods (2055 and 2085) were calculated. Then, the hourly data from the AEMET stations were modified based on the monthly temperature deltas obtained. The modification of hourly temperature data has been carried out according to methodologies already presented in other scientific works [28,51,52], based on which it is possible to apply the "a shift" algorithm to modify baseline climate data, to modify hourly baseline climate temperature values by adding the projected monthly average difference for future years. For this purpose, Equations (3) and (4) [42] have been used to calculate HDD and CDD, respectively, in the future; where $HDD_{d,Y}$ and $CDD_{d,Y}$—are daily values of HDD and CDD in the future; $T_{i,2018}$—temperature of measurements in i-hour of the day in the year 2018; ΔT^{j}_{Y-2018}—delta of monthly temperatures in j-month between years in future (Y = 2055 and 2085) and baseline climate.

$$HDD_{d,Y} = \left[\sum_{i=1}^{24} \left(T_b - (T_{i,2018} + \Delta T^{j}_{Y-2018}) \right)^{+} \right] \frac{1}{24} \tag{3}$$

$$CDD_{d,Y} = \left[\sum_{i=1}^{24} \left((T_{i,2018} + \Delta T^{j}_{Y-2018}) - T_b \right)^{+} \right] \frac{1}{24} \tag{4}$$

Based on the modified HDD and CDD results for the future, the WCS (Equation (1)) and SCS (Equation (2)) values for 2055 and 2085 were recalculated to account only for temperature changes without estimating changes in sunshine duration hours for the WCS index. This simplification was possible because the temperature in the climate models for the future already takes into account changes in atmospheric radiative conditions.

Finally, the WCS and SCS indices were calculated, and the dynamics of changes in the climate zones were obtained; for this purpose, the procedure followed for the calculation of the climate zone adaptation in the previous section was similar.

2.2.3. Proposed Update of Climate Zones for Peninsular Spain

The climatic zone classification for the 7967 Spanish municipalities of our research is based on determining their WCS and SCS indices.

Firstly, the computation of the WCS and SCS indices at the 77 weather stations as described above is carried out. It can be done by applying the formulae given because the values of temperature and sunshine duration hours required in the corresponding equations are available for those locations. These values are not available for the 7967 municipalities, and, as a consequence, their WCS and SCS indices cannot be calculated as done for the 77 weather stations. Their determination is then obtained by approximation, using an interpolation method based on radial basis functions (RBF).

For a given set of data (measurements and locations at which these measurements were obtained), the approximation procedure tries to determine a function ("approximating function") that is a good fit for the given data. In the approximation process using

interpolation, this good fit is achieved by imposing that the approximating function's outputs exactly match the given measurements at the corresponding locations. Besides, information on the studied problem can also be deduced at locations different from where the measurements were obtained [53].

Approximation, and in particular interpolation employing RBF, has found significant applications in science, engineering, economics, biology, and medicine, among others. In our case, the determination of the WCS and SCS indices at the 7967 municipalities from the WCS and SCS indices calculated at the 77 weather stations was obtained by using an approximant expressed as a finite linear combination of a particular radial basis function and its translations (it is important to emphasize that the selected 77 weather stations are well distributed throughout peninsular Spain). To make this approximation, the inverse multiquadric function is given by the expression $\phi(r) = \frac{1}{\sqrt{1+(\varepsilon r)^2}}, r \geq 0$, was chosen as the basis function, but there are other possibilities. A wide range of radial basis functions can be found in the literature [54]. The parameter $\varepsilon \geq 0$ that appears in the above expression is a shape parameter.

Let us illustrate the determination of the climatic severity indices more precisely. For the case of the WCS index, an interpolant function $s(x, y, z)$ given by the expression:

$$s(x, y, z) = \sum_{i=1}^{77} a_i \phi(\| (x, y, z) - (x_i, y_i, z_i) \|)$$

is considered, where $(x_i, y_i, z_i) \in \mathrm{R}^3$, $i = 1, \ldots, 77$, represent the latitude, longitude, and altitude coordinates at each of the 77 weather stations, $\|.\|$ is the Euclidean norm on R^3, $\phi: [0, \infty) \to \mathrm{R}$ is the basis function, and $a_i, i = 1, \ldots, 77$, constitutes a set of real coefficients to be determined.

These coefficients are obtained by imposing that the output provided by the interpolant function s at each of the weather stations is the corresponding WCS index, which is known. Once the coefficients are calculated, the interpolant function s is therefore determined. The evaluation of s at any value $(x, y, z) \in \mathrm{R}^3$ corresponding to the latitude, longitude, and altitude coordinates at any peninsular Spanish location provides the searched approximation for the unknown WCS index at that location. The SCS case would be analogous.

This is the procedure followed for the 2015–2018 period. The corresponding one for the years 2055 and 2085 is utterly similar except that, for the starting stage, the WCS and SCS indices at the 77 weather stations, both for the RCP 4.5 and RCP 8.5 contexts, need to be recalculated, as described in Section 2.2.2.

Once the WCS and SCS indices are obtained at each of the 7967 municipalities, they can be classified inside the corresponding climatic zone. Remarkably, the main advantage of the interpolation method previously exhibited is that it provides a continuous function to compute the climatic severity indices at any location. Consequently, it could make possible a numerical climatic classification at any municipality instead of the more rigid one described by zones.

2.2.4. Assessment of the Dynamics of Changes in Energy Demand in Dwellings

Once the WCS and SCS indices have been calculated for the periods 2015–2018, 2055, and 2085, an analysis of the dynamics of changes in energy demand is carried out for the RCP 4.5 and RCP 8.5 scenarios in the 77 locations of the meteorological stations selected for the study. The city of Madrid has been taken as a geographical reference point, to which, according to the CTE, the values WCS = 1.0 and SCS = 1.0 [42] correspond; consequently, by multiplying the value of the energy demand of a dwelling located in Madrid by the value of the WCS (or SCS) index of any geographical location, it is possible to estimate the demand of that dwelling in that place.

For this analysis, an existing typical building of a six-storey multi-family block of flats, used in the work of López–Ochoa et al. 2017 [55] was considered. The block consists of a ground floor and five storeys. Its base measures 22 by 22 m, which is equivalent to an area of 484 m^2. The height of each floor is 3 m. The main facade faces north. Each of the five floors has 4 types of flats: Apartment A has 3 bedrooms and a size of 100.05 m^2; Apartment B has 3 bedrooms and a size of 101.93 m; Apartment C has 4 bedrooms and a size of 137.64 m^2; and Apartment D has 3 bedrooms and a size of 103.69 m^2.

The building's thermal transmittances are similar to the limit values set in CTE-DB-HE1 2009, fulfilling the requirements of CTE-DB-HE 2009 [56]. The heating and cooling energy demands are assessed using the official HULC tool [39]. In addition to determine these demands, this tool is used to verify compliance with the requirements of CTE-DB-HE1 2013. The energy demand for heating this house in Madrid is 42.74 kWh/m^2 year and for cooling is 14.09 kWh/m^2 year [55].

3. Results and Discussion

After applying the previous section's methodological steps, the results shown in Figures 2–7 and Tables 3–5 were obtained, which are analyzed and discussed below.
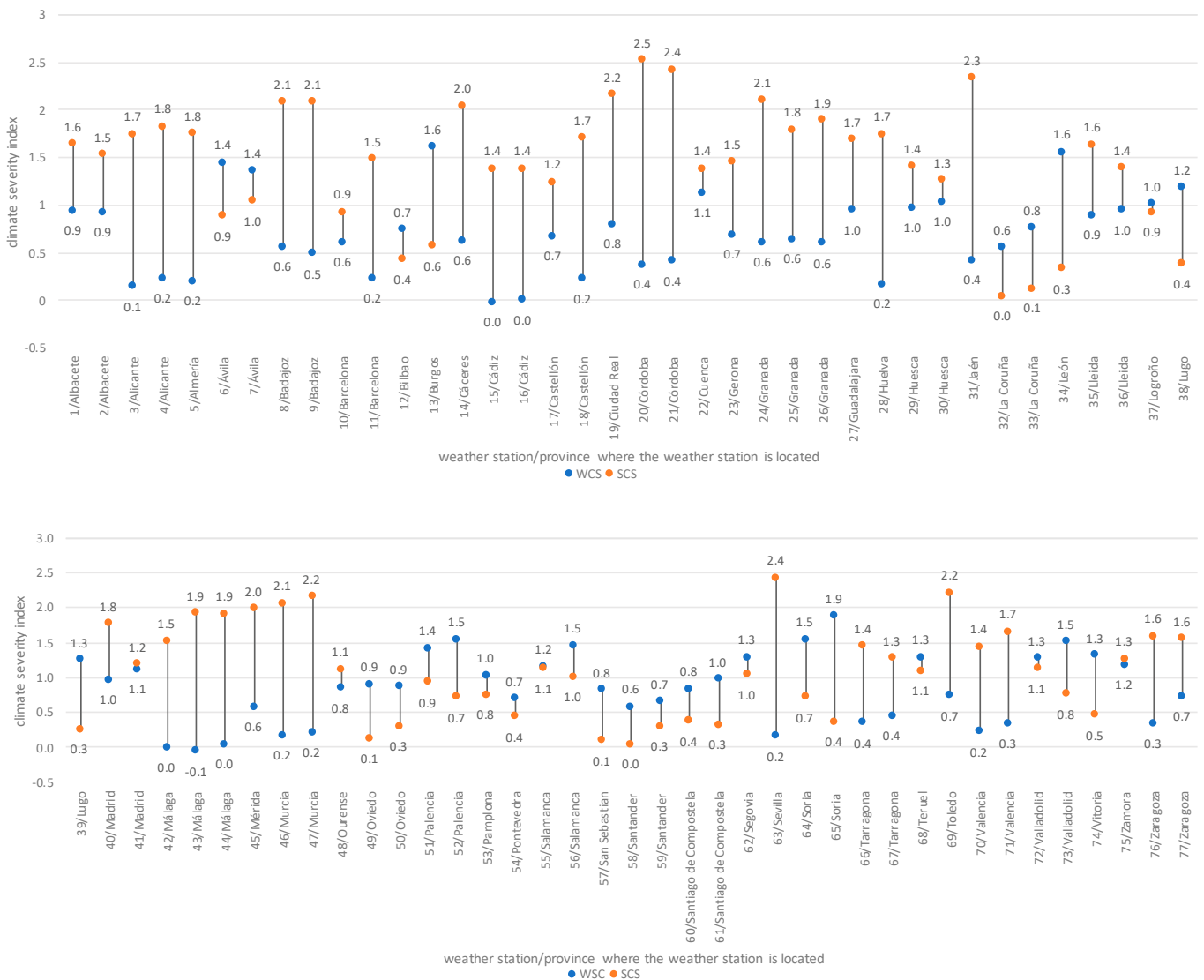

Figure 2. Calculated indices of winter (WCS) and summer (SCS) climate severity for the period 2015–2018.
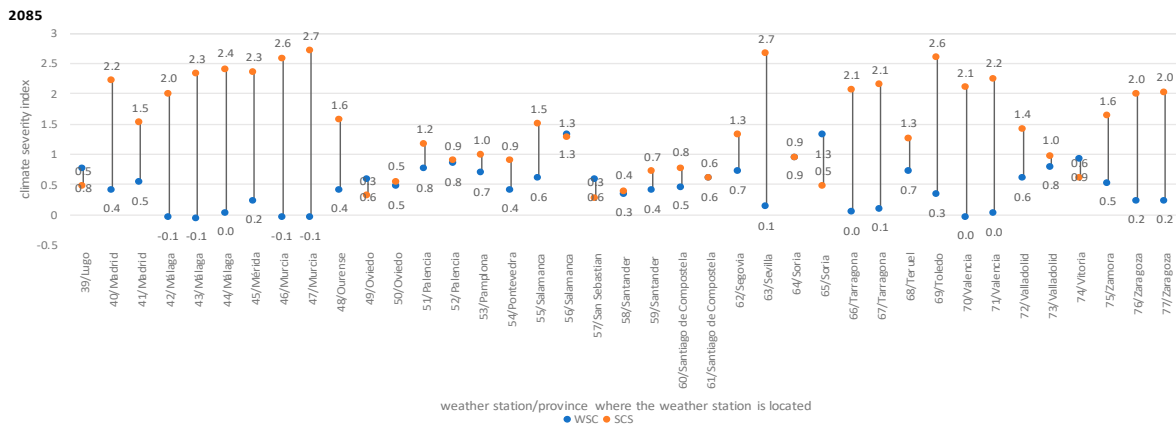
RCP 4.5 2055

2055

RCP 4.5 2085

2085

Figure 3. Calculated indices of winter (WCS) and summer (SCS) climate severity for the RCP 4.5.

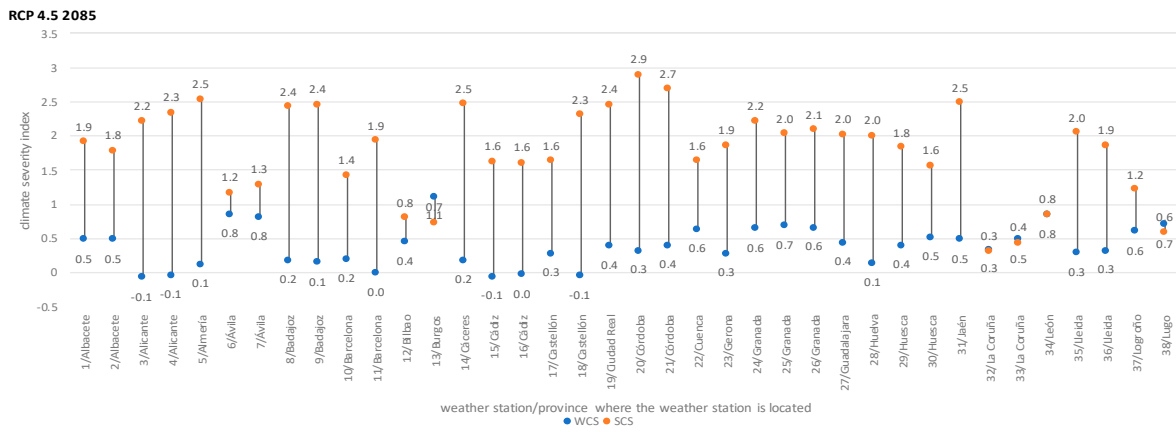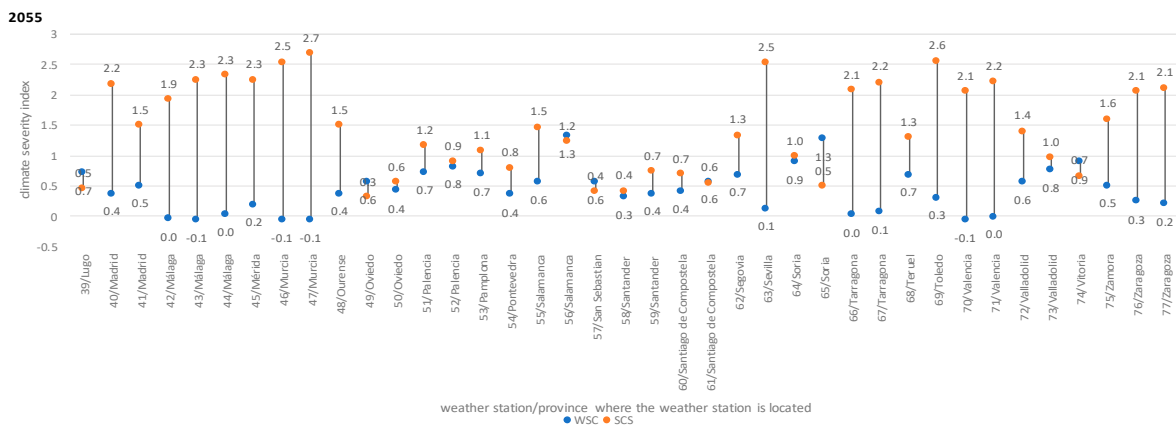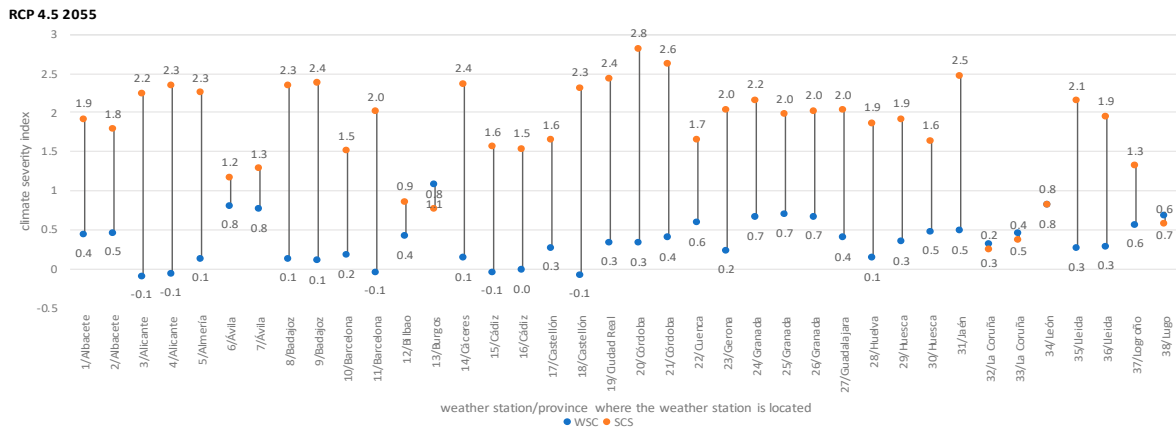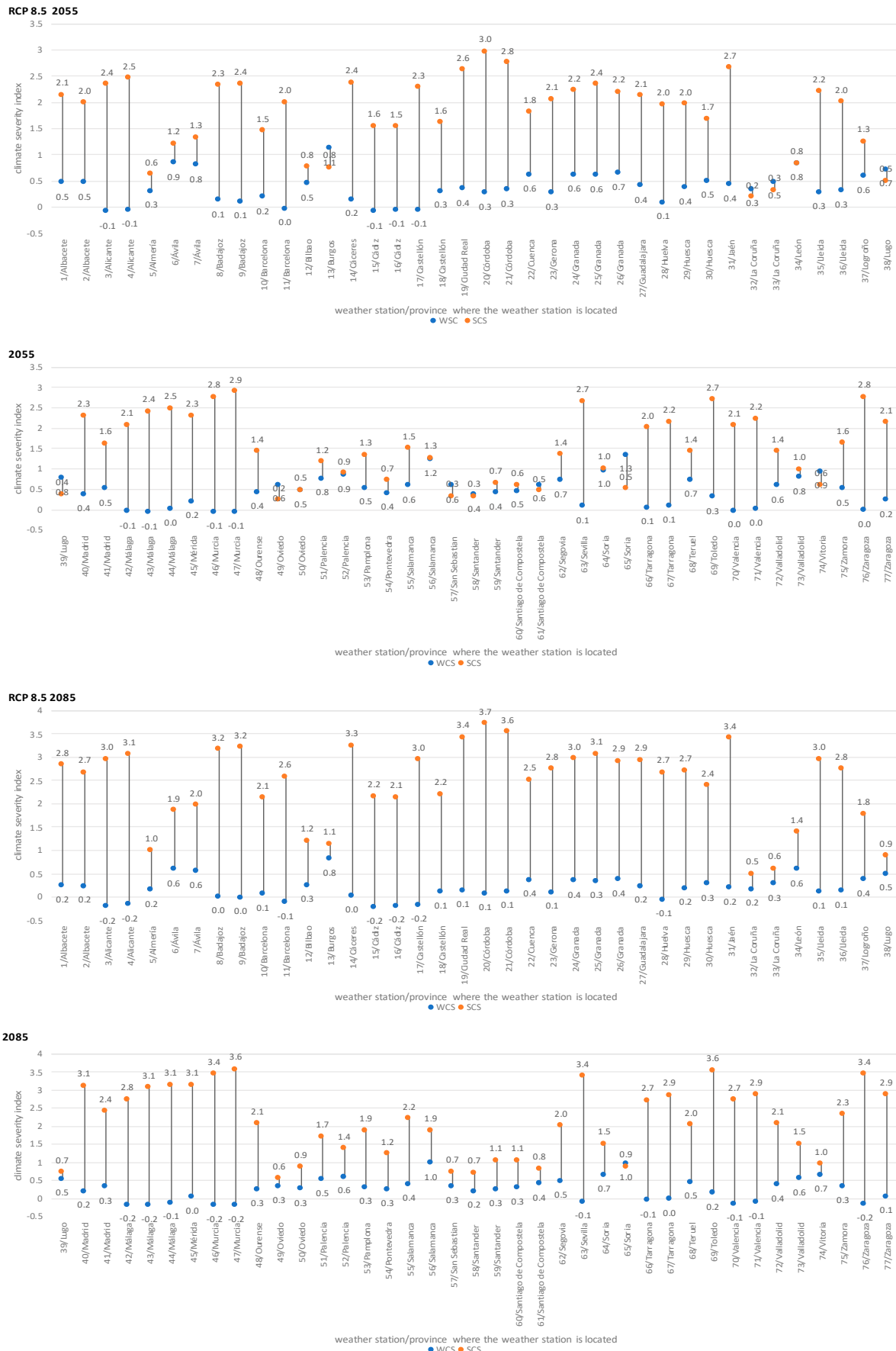**Figure 4.** Calculated indices of winter (WCS) and summer (SCS) climate severity for the RCP 8.5.
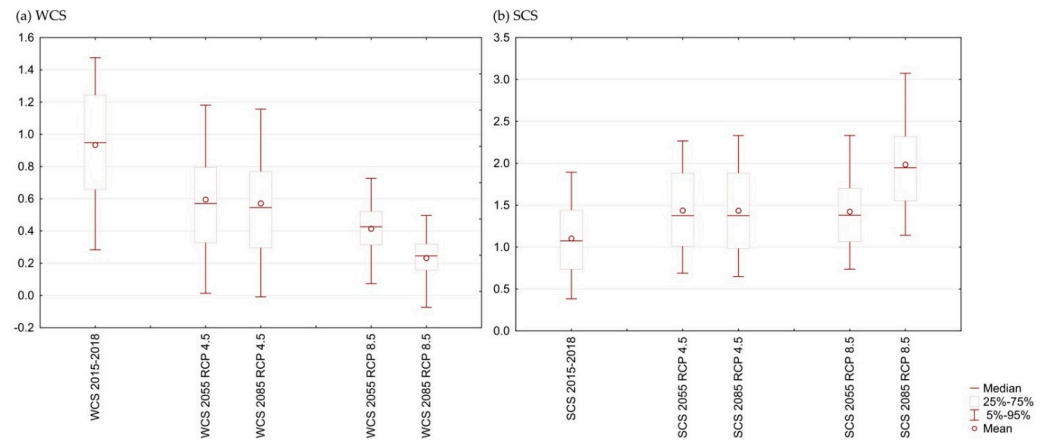
Figure 5. Boxplots of values of the WCS (**a**) and SCS (**b**) indexes in 7967 localities in mainland Spain for the period 2015–2018 and future periods.
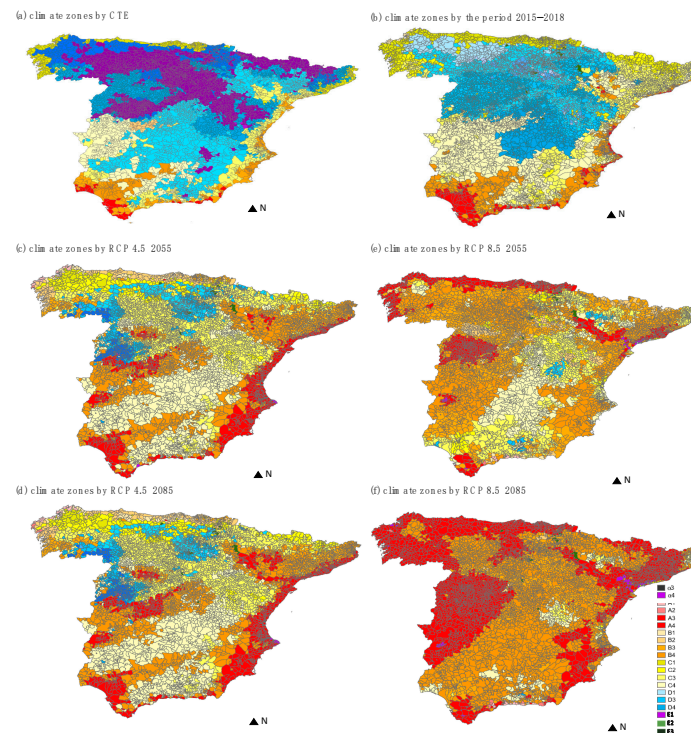
Figure 6. Maps of (**a**) CTE, (**b**) climatic zone by the period 2015–2018, (**c**) climate zones for RCP 4.5 2055, (**d**) climate zones for RCP 4.5 2085, (**e**) climate zones for RCP 8.5 2055, (**f**) climate zones for RCP 8.5 2085.
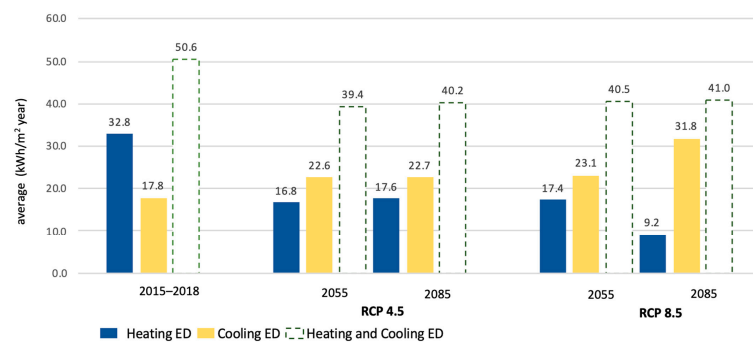
Figure 7. Dynamics of changes in the average of heating and cooling energy demand for the RCP 4.5 and RCP 8.5 scenarios by 77 stations.

Table 3. Dynamics of changes in climate zones according to scenarios.

Scenario	Winter Climatic Zone			Summer Climatic Zone			Winter + Summer Climatic Zone
	Code Number of CZ that Change	% of Cities Modifying CZ	% of Cities that Change CZ	Code Number of CZ that Change	% of Cities Modifying CZ	% of Cities that Change CZ	% of Cities that Change CZ
2015–2018	1	47.2%	52.1%	1	58.7%	72.0%	84%
	2	4.4%		2	12.2%		
	3	0.1%		3	0.2%		
	4	0.1%		4	0.0%		
	5	0.1%		−1	0.9%		
	−1	0.1%					
RCP 4.5 2055	1	44.8%	89.0%	1	47.7%	88.6%	98%
	2	40.5%		2	39.4%		
	3	3.0%		3	1.4%		
	4	0.0%		4	0.0%		
	5	0.0%		−1	0.1%		
	−1	0.7%					
RCP 4.5 2085	1	41.0%	89.9%	1	48.3%	87.6%	98%
	2	43.4%		2	38.1%		
	3	4.7%		3	1.2%		
	4	0.1%		4	0.0%		
	5	0.0%		−1	0.1%		
	−1	0.7%					
RCP 8.5 2055	1	24.4%	92.4%	1	33.0%	82.7%	97%
	2	33.1%		2	25.5%		
	3	26.5%		3	18.9%		
	4	4.1%		4	0.0%		
	5	0.0%		−1	4.1%		
	−1	3.8%					
RCP 8.5 2085	1	10.1%	100%	1	31.0%	91.0%	98%
	2	36.7%		2	26.3%		
	3	35.4%		3	32.2%		
	4	11.6%		4	0.0%		
	5	0.0%		−1	1.1%		
	−1	0.6%					

Table 4. Percentage of climate zones in different scenarios.

Climatic Zone	Present		RCP 4.5		RCP 8.5	
	CTE	2015–2018	2055	2085	2055	2085
Winter Climatic Zone						
α	0.00%	0.02%	0.15%	0.25%	0.41%	0.70%
A	0.74%	2.85%	12.89%	15.97%	16.62%	42.95%
B	5.47%	8.39%	29.21%	28.28%	53.39%	51.54%
C	20.05%	37.18%	43.54%	43.03%	28.28%	4.63%
D	44.90%	49.13%	11.60%	9.84%	1.27%	0.16%
E	28.76%	2.41%	2.59%	2.60%	0.01%	0.00%
Summer Climatic Zone						
1	40.05%	8.65%	1.41%	2.11%	0.99%	0.38%
2	22.80%	23.79%	10.53%	11.83%	8.11%	0.44%
3	28.58%	38.21%	38.54%	36.45%	41.02%	13.83%
4	8.55%	29.35%	49.51%	49.60%	49.84%	85.31%
Climatic Zone (Winter + Summer)						
α3	0.00%	0.01%	0.00%	0.00%	0.00%	0.00%
α4	0.00%	0.01%	0.15%	0.25%	0.41%	0.70%
A1	0.00%	0.00%	0.19%	0.23%	0.11%	0.18%
A2	0.00%	0.00%	0.04%	0.08%	0.01%	0.13%
A3	0.40%	0.13%	0.03%	0.14%	0.92%	2.82%
A4	0.34%	2.72%	12.64%	15.53%	15.54%	39.74%
B1	0.00%	0.19%	0.58%	1.04%	0.33%	0.04%
B2	0.00%	0.03%	3.00%	3.09%	5.35%	0.21%
B3	3.08%	0.65%	4.04%	4.31%	22.38%	9.62%
B4	2.40%	7.52%	21.57%	19.82%	25.26%	41.63%
C1	2.87%	5.57%	0.62%	0.77%	0.41%	0.11%
C2	3.21%	3.80%	4.10%	4.86%	2.45%	0.10%
C3	8.15%	13.93%	23.80%	23.89%	16.88%	1.37%
C4	5.81%	13.85%	14.90%	13.41%	8.50%	3.05%
D1	8.21%	2.42%	0.03%	0.08%	0.13%	0.05%
D2	19.58%	17.81%	3.26%	3.68%	0.30%	0.00%
D3	16.96%	23.49%	8.06%	5.51%	0.80%	0.03%
D4	0.00%	5.26%	0.25%	0.58%	0.04%	0.09%
E1	28.76%	0.39%	0.00%	0.00%	0.01%	0.00%
E2	0.00%	2.01%	0.05%	0.04%	0.00%	0.00%
E3	0.00%	0.01%	2.54%	2.55%	0.00%	0.00%

Table 5. Dynamics of changes in energy demand between significant seasons.

	RCP 4.5												
	2015–2018			**2055**			**Change**		**2085**			**Change**	
							ED between 2015–2018 and 2055					**ED between 2015–2018 and 2085**	
	ED			**ED**					**ED**				
	H	C	H + C	H	C	H + C	H	C	H	C	H + C	H	C
73	64.5	10.7	75.2	32.5	13.5	46.0	32.1	−2.8	33.8	13.5	47.3	30.8	−2.8
5	8.5	24.7	33.2	5.1	31.7	36.8	3.4	−7.0	4.7	35.5	40.2	3.8	−10.8
17	28.6	17.5	46.1	11.1	23.1	34.2	17.5	−5.6	11.5	22.8	34.4	17.1	−5.4
76	14.5	22.3	36.8	10.7	29.0	39.7	3.8	−6.8	9.4	27.9	37.3	5.1	−5.6

	RCP 8.5									
	2055			**Change**		**2085**			**Change**	
				ED between 2015−2018 and 2055					**ED between 2015−2018 and 2085**	
	ED					**ED**				
	H	C	H + C	H	C	H	C	H + C	H	C
73	33.8	13.8	47.6	30.8	−3.1	23.5	21.4	44.9	41.0	−10.7
5	12.8	8.9	21.7	−4.3	15.8	6.4	14.1	20.5	2.1	10.6
17	−2.1	32.3	30.1	30.8	−14.8	−7.3	41.6	34.3	35.9	−24.1
76	−0.9	39.0	38.2	15.4	−16.8	−6.4	48.5	42.1	20.9	−26.2

3.1. Determination of Climate Severity Indices

Figure 2 shows the values of the new climatic severities at the location of the 77 meteorological stations, according to the CTE calculation methodology, and taking into account the climatic conditions of the period 2015–2018.

It is observed that the WCS index values range between −0.06 and 1.87, determined for the coastal province of Malaga (station #43) and Soria (station #65), respectively. The three negative WCS values recorded, one case with a value of 0, or positive but shallow values, below 0.4, have occurred in regions with mild winters; this is the case of the station above #43, located in Málaga, #15 and #42, located in Cádiz and Málaga respectively, or stations #4 (Alicante), #11 (Barcelona), #16 (Cádiz), #18 (Castellón), #28 (Huelva), #44 (Málaga), #66 (Tarragona), and #70 (Valencia), among others, all of the coastal areas in the south of the peninsula or the Mediterranean area. In these cases, a good design of the building's constructive solutions will allow the indoor comfort temperature to be reached without implementing active heating systems. On the contrary, the higher the WSC value, the lower the winter temperatures in these regions, which leads to higher heating energy demands. This is the case of stations #6 and #7 located in Avila, #13 in Burgos, #52 in Palencia, #56 in Zamora, and #64 and #65 in Soria, all of them with WSC values higher than 1.35 and located in the north of the peninsula, in provinces with shallow temperatures.

In the case of the SCS, values reaching the minimum in the coastal province of La Coruña (station #32), with 0.04, and the maximum in the inland province of Cordoba (station #20), with 2.52, are observed. The lowest SCS values occur in regions with cool summer temperatures; this is the case of stations #32, #33, #60, and #61 located in La Coruña, #34 in León, #49 and #50 in Asturias, #57 in Guipúzcoa, #58 and #59 in Cantabria, among others, all of them in the north of the peninsula and with SCS values below 0.4. In these regions, with a good design of the building's constructive solutions, the indoor comfort temperature can be reached without implementing active cooling systems. However, the higher the SCS value, the higher the summer temperatures in these regions, which leads to higher cooling energy demands. It is the case of stations located in the peninsula's interior, with SCS values higher than 2, such as #8 and #9 in Badajoz, #14 in Cáceres, #19 Ciudad Real, or #20 and #21 in Córdoba, among others.

The stations located in the inland provinces of Madrid (#40, #41), Salamanca (#55, #56), or Segovia (#62) stand out, with WCS and SCS values higher than 1. These conditions are found in places with a Mediterranean climate far from the sea, with long and cold winters, with temperatures that can drop below 0 °C, with numerous frosts occurring at night. In contrast, summers are pretty hot and dry, with a temperature range of 18.5 °C, and temperatures often exceed 30 °C. In these regions, the energy demand is considerably higher than in coastal areas, both in summer and winter, where the need for passive strategies to reduce energy consumption is essential. Thus, building solutions with high thermal inertia could be an effective mechanism to achieve thermal comfort [57].

Finally, comparing the climate severity values of the different station locations in an area shows significant temperature contrasts between the urban and metropolitan regions, for example, the case in Barcelona, where station #11, located in the city center and close to the sea coast, resulted in climatic severities of WCS = 0.23 and SCS = 1.48, while station #10, located outside the city center, showed significantly different values (with WCS = 0.61 and SCS = 0.92). The same is true for the stations in Valladolid, where station #72, located in the city center, resulted in climatic severities of WCS = 1.27 and SCS = 1.12 while station #73, located outside the city center, showed considerably different values (with WCS = 1.51 and SCS = 0.76). These results highlight the urban heat island effect, a phenomenon of thermal origin that occurs in urban areas and consists of a different temperature, which tends to be higher, especially at night, in the center of cities due to massive building [58].

3.2. Determination of the Dynamics of Changes in Climate Severity Indices

Figures 3 and 4 show the results obtained from calculating the WCS and SCS indices for the years 2055 and 2085, under the RCP 4.5 and RCP 8.5 climate change scenarios at the 77 reference stations.

For the RCP 4.5 scenario (Figure 3), it is observed that the WCS index values for 2055 range between −0.1 and 1.3, determined for the stations located in the Mediterranean coastal cities of Alicante, Barcelona, Cádiz, Castellón, Málaga, Murcia, and Valencia and the inland city of Soria, respectively. Thus, the projected emissions for this scenario mean that by mid-century, all the reference stations will be in regions with mild winters, which will lead to a drastic drop in heating consumption. It is observed that the SCS will be increasing in the first half of the 21st century, with values ranging between 0.3 and 2.8 for the cities of Oviedo (station #49) and Cordoba (station #20). It will imply a significant increase in summer temperatures, which will drastically increase cooling consumption. However, by the climate trends projected for this scenario, a progressive stabilization of temperatures at all stations will be observed by 2085. Thus, by the end of the century, WCS values range between −0.1 and 1.3; SCS values range between 0.3 and 2.9.

For the RCP 8.5 scenario (Figure 4), a more drastic change in WCS and SCS values is observed than in the previous scenario. Thus, the WCS index values for 2055 range from −0.1 to 1.4 and decrease until 2085, with values ranging from −0.1 to 1.1. In SCS, a progressive increase is observed until 2055, to increase dramatically until 2085, with values ranging between 0.2 and 3 and 0.5 and 3.7. It reflects by the end of the century and increases in cooling energy demands and an almost total decrease in heating energy demands in most cities of the reference seasons.

3.3. Proposed Update of Climate Zones for Peninsular Spain

Based on the climate severities calculated from the 77 meteorological stations for 2015–2018 and the RCP 4.5 and 8.5 scenarios, the climate severities for the period 2015–2018 and the years 2055 and 2085 for 7967 localities in peninsular Spain have been obtained using approximation techniques. Based on Table 1, the climatic zones of the 7967 localities have been identified. The results are described in Figures 5 and 6 and Tables 3 and 4 below.

3.3.1. Climate Severities for 2015–2018 and the Periods 2055 and 2085 of the RCP 4.5 and 8.5 Scenarios for 7967 Locations in Mainland Spain

Figure 5 shows the average WCS and SCS values for 2015–2018 and 2055 and 2085 for RCP 4.5 and 8.5. Comparing the values obtained for the WCS indices with those for the 2015–2018 range (Figure 5a) shows that, for the RCP 4.5 scenario, the average value decreases considerably from 0.96 in 2015–2018 to 0.57 and 0.56 in 2055 and 2085, respectively. It is because emissions in this scenario peak around 2040 and then stabilize. In the RCP 8.5 scenario, the decrease is more significant, with average values of 0.43 and 0.28 for 2055 and 2085, respectively, due to the more abrupt character of this scenario, where the most significant changes are located to the end of the 21st century. For both scenarios, there is a significant softening of winter temperatures [1].

For the SCS indices, the comparison with the values obtained in the 2015–2018 interval (Figure 5b) shows that, for the RCP 4.5 scenario, the average value increases from 1.15 in 2015–2018 to 1.43 in 2055; it then stabilizes until 2085 with 1.45. In the RCP 8.5 scenario for 2055, compared to 2015–2018, a slight increase is observed with 1.43 before rising sharply to 1.93 by 2085. The most pessimistic climate change projection will lead to more noticeable temperature changes, with sweltering summers.

Finally, it should be noted that it is not possible to compare these indices with current regulations since the CTE does not provide exact values, which leads to problems in the field of energy efficiency research and adaptation to climate change in buildings in Spain.

3.3.2. Proposed Update of Climate Zones for Peninsular Spain

Once the WCS and SCS of the 7967 localities for the period 2015–2018 and the RCP 4.8 and 8.5 scenarios have been obtained, based on Table 1, the new climate zones of the 7967 localities of peninsular Spain have been obtained. Figure 6 shows the geographical distribution of the CTE climate zones for 2015–2018 and the RCP 4.5 and 8.5 scenarios. To analyze the variation of the climate rating observed concerning the CTE, Table 3 shows the percentage of cities that vary this rating, while Table 4 shows the percentage of climate zones in the CTE in the period 2015–2018 and the RCP 4.5 and 8.5 scenarios. The results obtained are discussed below.

Proposed Update of Climate Zones for Peninsular Spain for the Period 2015–2018

Concerning the CTE in 2015–2018 (Table 3), more than 80% of the cities have already changed their climate zone (winter + summer). Moreover, this change has meant that the number of climate zones in the country has increased from the 12 contemplated in the CTE to 19, with seven new zones appearing that were not previously re-categorized (α3, α4, B1, B2, D4, E1, and E2) (Table 4). The appearance of zones α3 and α4 should be highlighted, highlighting the trend, in areas such as the Mediterranean, towards climates more characteristic of subtropical zones.

In the case of winter, approximately half of the cities have changed their winter climate zone to a warmer zone compared to the CTE (Table 3), although the most significant changes occur in the south and on the Mediterranean coast, while the climate zones in the north, northwest, southwest, and eastern part of Andalusia remain unchanged (Figure 6a,b). The winter climate zone D (Table 4) stands out, present in 49% of the localities, making it the predominant one. This result shows a rise in winter temperatures in almost half of the territory concerning what is contemplated in the current regulations. The average increase in temperatures is causing a decrease in the energy demand for heating but implies that the limits of parameters such as transmittance are compromised.

In summer climate zones, more drastic changes are observed, especially on the Mediterranean coast (Figure 6a,b), due to the intense summer warming of the Mediterranean inland waters in recent years [59]. Thus for 2015–2018, 72% of cities have changed their summer CZs to warmer ones than those reported in the CTE (Table 3). Specifically, 58.7% and 12.2% of localities have changed their summer CZ to 1 and 2 warmer ratings, respectively. Climate zones 3 and 4 are the most predominant present in 38.21% and 29.35% of the localities (Table 4).

Proposed Climate Zones for Peninsular Spain for the RCP 4.5 Scenario Projections

Under the RCP 4.5 scenario (Table 3) for 2055 and 2085, 98% of the cities will see their climate zone (winter + summer) change concerning the CTE. Furthermore, Figure 6c,d shows how the geographical distribution of climate zones for 2085 resembles the resulting distribution for 2055. These climate zone changes are a consequence of the closeness of absolute values of WCS and SCS to the limiting value of climate zone delimitation (Table 1) so that a minimal change of the index can lead to a change of climate zone for a locality. This result is a limiting factor in the zoning of the existing CTE, reinterpreting the need for a significant improvement in the development and methodology of the current regulations in force.

As shown in Figure 6c,d, by 2055 and 2085, half of the Mediterranean coastal localities will fall into climate zone A4. These regions will be characterized by hotter summers and warmer winters, while the northern coastal cities will have a greater variety of climate zones over the century, with mild summer temperatures and colder winters. The same occurs in the peninsula's interior, where a heterogeneous distribution is observed due to the complexity of the relief and the diversity of mesoclimatic and microclimatic zones. Thus, by 2085, 23.89% and 19.82% of the localities will have a C3 and B4 climate classification, while the coldest climate zones will disappear (Table 4).

In winter CZs (Table 3), for the periods 2055 and 2085, practically 90% of the localities will change their climate zoning compared to that retained in the CTE. Specifically, for the period 2055, 44.8% of the localities will change their zoning to a warmer one and 40.5% of the localities to two warmer zones. Similarly, by 2085, 41%, 43.4%, and 4.7% of localities will change their winter rating to 1, 2, and 3 warmer zones, respectively. Thus, the geographical distribution of winter climate zones for 2085 resembles the resulting distribution for 2055, where only 8% of cities will observe zone changes between these two years. The increase of the A rating concerning the CTE (Figure 6c,d and Table 4), from 0.74% in the CTE to 12.89% and 15.97% in 2055 and 2085, respectively, stands out. In contrast, the E rating decreases drastically from 28.76% in the CTE to only 2.6% in 2085. These results again show that the trend towards warmer and warmer areas will continue throughout the century.

In the summer CZ case (Table 3), for the periods 2055 and 2085, 88.6% and 87.6% of the locations will change their climate zonation compared to the CTE. By 2055, 47.7% of localities will change their zoning to a warmer one, and 39.4% of localities will change their zoning to two warmer zones. Similarly, by 2085, 48.3% and 38.1% of localities will change their summer rating to 1 and 2 warmer zones, respectively. As in the winter season, the differences between 2055 and 2085 are not significant. Although, throughout this scenario, there is a significant increase in rating 4 in the localities concerning the CTE (Figure 6c,d and Table 4), from 8.55% in the CTE to 49.51% and 49.60% in 2055 and 2085, respectively. In contrast, rating 1 decreases drastically from 40.05% in the CTE to only 2.11% in 2085. These results demonstrate the need to develop new summer zones within rating 4, with the consequent improvement in terms of building recommendations.

Proposed Climate Zones for Peninsular Spain for the RCP 8.5 Scenario Projections

Under the RCP 8.5 scenario (Table 3) for 2055 and 2085, a drastic increase in the change of climate zone classification (winter + summer) concerning the CTE is foreseen, showing that 98% of the cities will be affected. Furthermore, Figure 6e,f shows that the geographical distribution of climate zones for 2085 will undergo a significant dynamism, with zones A4 and B4, with 39.74% and 41.63%, dominating the peninsula. These zones are characterized by mild winters and sweltering summers, leading the peninsula to have climates more typical of tropical regions by the end of the century.

In the winter CZs (Table 3), for the periods 2055 and 2085, 92.4% and 100% of the locations will change their climate zoning compared to the CTE. Specifically for the period 2055, 24.4, 33.1, and 26.5% of the localities will change their qualification by one, two, and three warmer zones, respectively. Similarly, by 2085, 10.1, 36.7, and 35.4% of localities will change their winter rating to one, two, and three warmer zones, respectively. Through-

out this scenario, there is a significant increase in the presence of the A and B rating in the localities concerning the CTE (Table 4), from 0.74 and 5.47% in the CTE to 42.95 and 51.54% in 2085, respectively, on the contrary, the C and D ratings decrease drastically, while the E climate zone disappears entirely by 2085. These results are due to the already indicated trend towards warmer and warmer zones.

In the summer CZ case (Table 3), for the periods 2055 and 2085, 82.7% and 91% of the localities will change their climate zoning compared to the CTE. By 2055, 33% of the localities will change their zoning to a warmer one, 25.5% of the localities to two warmer zones, and 18.9% to three warmer zones. Similarly, by 2085, 31%, 26.3%, and 32.2% of localities will change their summer rating to 1, 2, and 3 warmer zones, respectively. In Figure 6e,f, significant differences are observed between 2055 and 2085. Throughout this scenario, there is a significant increase in the presence of rating 4 in the localities concerning the CTE (Table 4), from 8.55% in the CTE to 49.84% and 85.31% in 2055 and 2085, respectively, in contrast, rating 1 decreases drastically from 40.05% in the CTE to only 0.38% in 2085. These results show that more than half of the buildings designed with zone E's technical requirements will not comply with the regulations in less than 25 years.

3.4. Analysis of the Dynamics of Dhanges in Energy Demand for RCP 4.5 and RCP 8.5 Scenarios

In order to a analyze the effects that the observed climate dynamism will have on the energy demand of buildings, Figure 7 shows the average results of the estimated change in energy demand for heating and cooling, calculated based on the definition of the WCS and SCS indices of the 77 stations, for the typical building used for 2015–2018 and the RCP 4.5 and RCP 8.5 scenarios. Besides, Table 5 shows the estimated energy demand for heating and cooling, for four significant stations, for the building type used for 2015–2018 and the RCP 4.5 and RCP 8.5 scenarios.

In the RCP 4.5 scenario (Figure 7), by the year 2055, the energy demand of the 77 stations is expected to decrease by an average of 11.23 kWh/m^2 year compared to 2015–2018. Specifically, heating demand will decrease by an average of 16 kWh/m^2 year, with the most significant decreases observed in stations located in mountainous areas at 900 meters above sea level; this is due to the notable effect of the continental climate, which will see its meteorological conditions soften in winter due to the effects of climate change. Such is the case of station 73, located in Valladolid, with a reduction of 32 kWh/m^2 year. However, cooling demand will increase by an average of 4.8 kWh/m^2 year, compared to 2015–2018, in cities located in the southeast, characterized by a semi-arid climate; specifically, station 5, located in the city of Almeria with an increase in cooling energy demand by 2055 of 7.045 kWh/m^2 year compared to 2015–2018. However, due to this climate scenario's stabilizing nature between 2055 and 2085, no significant differences are observed between the average demand values for heating and cooling, with an average increase of only 0.8 kWh/m^2 year.

Under the RCP 8.5 scenario (Figure 7), by the year 2055, heating and cooling energy demand for all seasons are expected to decrease by an average of 10 kWh/m^2 year compared to 2015–2018. Specifically, heating demand will decrease by an average of 15.4 kWh/m^2 year, highlighting station 17, located in the city of Castellón, where a high reduction value, estimated at 30 kWh/m^2 year, is foreseen. In contrast, cooling demand will increase by an average of 5.3 kW/m^2 year compared to 2015–2018. Station 76, located in Zaragoza, stands out in particular, with an increase in cooling energy demand by 2055 of 16.7 kWh/m^2 year compared to 2015–2018. It should be noted that, unlike the RCP 4.5 scenario, under the RCP 8.5 scenario, there are significant differences between 2055 and 2085. Thus, by 2085, the average heating energy demand will decrease by 8.2 kWh/m^2 year, while the cooling demand will increase by 8.7 kWh/m^2 year compared to 2055. This trend is localized in cities located in the southwestern, southern and Mediterranean coastal parts of the country. These results are explained by expanding the semi-arid climate that the south and southeast coast will undergo under this scenario, where summers will be hotter and drier, significantly increasing the energy demand of dwellings for cooling. This increase will also be affected by the additional thermal effect of the Mediterranean Sea's warming surface waters.

4. Conclusions

In this work, the climatic zones of all the cities of peninsular Spain have been updated. The results show that the allocation of climatic zones currently included in the CTE is not suitable for current and future climatic conditions. Given the importance of precision in the assignment of a climatic zone when correctly sizing domestic hot water, heating and cooling systems, and the appropriate selection of the construction materials used, this situation jeopardizes the achievement of truly sustainable buildings. Specifically, taking into account the climate data recorded in the 2015–2018 period, 80% of cities today have a different climate zone to that of the CTE; moreover, it is expected that by the year 2085 and under the forecasts recorded in the RCP 4.5 and RCP 8.5 scenarios, practically all cities in mainland Spain will change their climate zone to warmer ones.

This significant climate change that the region under study is already undergoing will help reduce the heating energy demand of dwellings and increase the demand for cooling. Therefore, architectural and construction standards must adapt to the urban environment's actual conditions and consider the main scenarios to lead to a building design that mitigates climate change and adapts to them. It intensifies the need to develop new climate zones and build recommendations to preserve future periods' correct thermal conditions.

Finally, it should be noted that the consequences observed in peninsular Spain can be extrapolated to other areas so that the methodology proposed in this work can be extended to any region, making a significant scientific contribution in terms of reflection on the current capacities and possibilities for improvement of the building stock.

Author Contributions: Conceptualization, C.D.-L., J.J., K.V., M.L.R., M.C. and M.Z.; Data curation, J.J., K.V. and M.L.R.; Formal analysis, C.D.-L., K.V. and M.Z.; Acquisition financing, M.C. and M.Z.; Research, C.D.-L., J.J., K.V., M.L.R., M.C. and M.Z.; Methodology, J.J., K.V., M.L.R. and M.Z.; Project administration, M.Z.; Resources, C.D.-L., M.C. and M.Z.; Software, J.J. and M.L.R.; Supervision, M.Z.; Validation, J.J., K.V., M.L.R. and M.Z.; Writing—original draft, C.D.-L., J.J., K.V., M.L.R., M.C. and M.Z.; Writing—revision and editing, C.D.-L., J.J., K.V., M.L.R., M.C. and M.Z. All authors have read and agreed to the published version of the manuscript.

Institutional Review Board Statement: Not applicable.

Informed Consent Statement: Not applicable.

Data Availability Statement: Data are provided upon request to the corresponding author.

Conflicts of Interest: The authors declare no conflict of interest.

Abbreviations

AdapteCCa	Climate Change Adaptation Platform
AEMET	State Meteorological Agency
C	cooling energy demand
CDD	cooling degree-days
CSI	climatic severity index
CTE	Technical Building Code
CZ	climate zone
DB-HE	Basic Document on Energy Saving
EC	energy consumption
ED	energy demand
ESRL	Earth System Research Laboratory
GDP	Gross Domestic Product

H	heating energy demand
HDD	heating degree-days
IPCC	Intergovernmental Panel on Climate Change
LLGHG	long-lived greenhouse gas emissions
RBF	radial basis functions
RF	Radiative Forcing
RCP	Representative Concentration Pathways
SCS	severity index for summer
WCS	severity index for winter
WS	Weather station

References

1. IPCC. *Climate Change 2014: Synthesis Report. Contribution of Working Groups I, II and III to the Fifth Assessment Report of the Intergovernmental Panel on Climate Change*; Core Writing Team, Pachauri, R.K., Meyer, L.A., Eds.; IPCC: Geneva, Switzerland, 2014; 151p.
2. Houghton, J.T.; Ding, Y.D.J.G.; Griggs, D.J.; Noguer, M.; van der Linden, P.J.; Dai, X.; Johnson, C.A. *Climate Change 2001: The Scientific Basis*; The Press Syndicate of the University of Cambridge: Cambridge, UK, 2001; p. 881. [CrossRef]
3. Chuwah, C.; Van Noije, T.; Van Vuuren, D.P.; Hazeleger, W.; Strunk, A.; Deetman, S.; Beltran, A.M.; Van Vliet, J. Implications of Alternative Assumptions Regarding Future Air Pollution Control in Scenarios Similar to the Representative Concentration Pathways. *Atmos. Environ.* **2013**, *79*, 787–801. [CrossRef]
4. Verichev, K.; Zamorano, M.; Carpio, M. Effects of Climate Change on Variations in Climatic Zones and Heating Energy Consumption of Residential Buildings in the Southern Chile. *Energy Build.* **2020**, *215*, 109874. [CrossRef]
5. Thomson, A.M.; Calvin, K.V.; Smith, S.J.; Kyle, G.P.; Volke, A.; Patel, P.; Delgado-Arias, S.; Bond-Lamberty, B.; Wise, M.A.; Clarke, L.E.; et al. RCP 4.5: A Pathway for Stabilization of Radiative Forcing by 2100. *Clim. Chang.* **2011**, *109*, 77–94. [CrossRef]
6. Riahi, K.; Rao, S.; Krey, V.; Cho, C.; Chirkov, V.; Fischer, G.; Kindermann, G.; Nakicenovic, N.; Rafaj, P. RCP 8.5—A Scenario of Comparatively High Greenhouse gas Emissions. *Clim. Chang.* **2011**, *109*, 33–57. [CrossRef]
7. Lorusso, A.; Maraziti, F. Heating System Projects Using the Degree-Days Method in Livestock Buildings. *J. Agric. Eng. Res.* **1998**, *71*, 285–290. [CrossRef]
8. Troup, L.; Eckelman, M.J.; Fannon, D. Simulating Future Energy Consumption in Office Buildings Using an Ensemble of Morphed Climate Data. *Appl. Energy* **2019**, *255*, 113821. [CrossRef]
9. Bellia, L.; Mazzei, P.; Palombo, A. Weather Data for Building Energy Cost-Benefit Analysis. *Int. J. Energy Res.* **1998**, *22*, 1205–1215. [CrossRef]
10. Grøntoft, T. Climate Change Impact on Building Surfaces and Façades. *Int. J. Clim. Chang. Strat. Manag.* **2011**, *3*, 374–385. [CrossRef]
11. Nik, V.M.; Mundt-Petersen, S.; Kalagasidis, A.S.; De Wilde, P. Future Moisture Loads for Building Facades in Sweden: Climate Change and Wind-Driven Rain. *Build. Environ.* **2015**, *93*, 362–375. [CrossRef]
12. Brown, M.A.; Cox, M.; Staver, B.; Baer, P. Modeling climate-driven changes in U.S. buildings energy demand. *Clim. Chang.* **2016**, *134*, 29–44. [CrossRef]
13. Christenson, M.; Manz, H.; Gyalistras, D. Climate warming impact on degree-days and building energy demand in Switzerland. *Energy Convers. Manag.* **2006**, *47*, 671–686. [CrossRef]
14. De Rosa, M.; Bianco, V.; Scarpa, F.; Tagliafico, L.A. Heating and cooling building energy demand evaluation; a simplified model and a modified degree days approach. *Appl. Energy* **2014**, *128*, 217–229. [CrossRef]
15. Dolinar, M.; Vidrih, B.; Kajfež-Bogataj, L.; Medved, S. Predicted changes in energy demands for heating and cooling due to climate change. *Phys. Chem. Earth Parts A/B/C* **2010**, *35*, 100–106. [CrossRef]
16. Jylhä, K.; Jokisalo, J.; Ruosteenoja, K.; Pilli-Sihvola, K.; Kalamees, T.; Seitola, T.; Mäkelä, H.M.; Hyvönen, R.; Laapas, M.; Drebs, A. Energy demand for the heating and cooling of residential houses in Finland in a changing climate. *Energy Build.* **2015**, *99*, 104–116. [CrossRef]
17. Berardi, U.; Jafarpur, P. Assessing the impact of climate change on building heating and cooling energy demand in Canada. *Renew. Sustain. Energy Rev.* **2020**, *121*, 109681. [CrossRef]
18. da Guarda, E.L.A.; Domingos, R.M.A.; Jorge, S.H.M.; Durante, L.C.; Sanches, J.C.M.; Leão, M.; Callejas, I.J.A. The influence of climate change on renewable energy systems designed to achieve zero energy buildings in the present: A case study in the Brazilian Savannah. *Sustain. Cities Soc.* **2020**, *52*, 101843. [CrossRef]
19. Hekkenberg, M.; Moll, H.; Uiterkamp, A.S. Dynamic temperature dependence patterns in future energy demand models in the context of climate change. *Energy* **2009**, *34*, 1797–1806. [CrossRef]
20. Seljom, P.; Rosenberg, E.; Fidje, A.; Haugen, J.E.; Meir, M.; Rekstad, J.; Jarlset, T. Modelling the effects of climate change on the energy system—A case study of Norway. *Energy Policy* **2011**, *39*, 7310–7321. [CrossRef]
21. Belzer, D.B.; Scott, M.J.; Sands, R.D. Climate Change Impacts on U.S. Commercial Building Energy Consumption: An Analysis Using Sample Survey Data. *Energy Sources* **1996**, *18*, 177–201. [CrossRef]

22. Amato, A.D.; Ruth, M.; Kirshen, P.; Horwitz, J. Regional Energy Demand Responses to Climate Change: Methodology and Application to the Commonwealth of Massachusetts. *Clim. Chang.* **2005**, *71*, 175–201. [CrossRef]
23. Xu, P.; Huang, Y.J.; Miller, N.; Schlegel, N.; Shen, P. Impacts of climate change on building heating and cooling energy patterns in California. *Energy* **2012**, *44*, 792–804. [CrossRef]
24. Asimakopoulos, D.; Santamouris, M.; Farrou, I.; Laskari, M.; Saliari, M.; Zanis, G.; Giannakidis, G.; Tigas, K.; Kapsomenakis, J.; Douvis, C.; et al. Modelling the Energy Demand Projection of the Building Sector in Greece in the 21st Century. *Energy Build.* **2012**, *49*, 488–498. [CrossRef]
25. Olonscheck, M.; Holsten, A.; Kropp, J.P. Heating and Cooling Energy Demand and Related Emissions of the German Residential Building Stock under Climate Change. *Energy Policy* **2011**, *39*, 4795–4806. [CrossRef]
26. Zhai, Z.J.; Helman, J.M. Implications of Climate Changes to Building Energy and Design. *Sustain. Cities Soc.* **2019**, *44*, 511–519. [CrossRef]
27. Shi, Y.; Wang, G. Changes in Building Climate Zones over China Based on High-Resolution Regional Climate Projections. *Environ. Res. Lett.* **2020**, *15*, 114045. [CrossRef]
28. Belcher, S.; Hacker, J.; Powell, D. Constructing Design Weather Data for Future Climates. *Build. Serv. Eng. Res. Technol.* **2005**, *26*, 49–61. [CrossRef]
29. Dodoo, A.; Gustavsson, L.; Bonakdar, F. Effects of Future Climate Change Scenarios on Overheating Risk and Primary Energy Use for Swedish Residential Buildings. *Energy Procedia* **2014**, *61*, 1179–1182. [CrossRef]
30. Roux, C.; Schalbart, P.; Assoumou, E.; Peuportier, B. Integrating Climate Change and Energy Mix Scenarios in Lca Of Buildings and Districts. *Appl. Energy* **2016**, *184*, 619–629. [CrossRef]
31. Sailor, D.J. Risks of Summertime Extreme Thermal Conditions in Buildings as a Result of Climate Change and Exacerbation of Urban Heat Islands. *Build. Environ.* **2014**, *78*, 81–88. [CrossRef]
32. Guan, L. Preparation of Future Weather Data to Study the Impact of Climate Change on Buildings. *Build. Environ.* **2009**, *44*, 793–800. [CrossRef]
33. Wang, X.; Chen, D.; Ren, Z. Assessment of Climate Change Impact on Residential Building Heating and Cooling Energy Requirement in Australia. *Build. Environ.* **2010**, *45*, 1663–1682. [CrossRef]
34. Andrić, I.; Gomes, N.; Pina, A.; Ferrão, P.; Fournier, J.; Lacarrière, B.; Le Corre, O. Modeling the Long-Term Effect Of Climate Change on Building Heat Demand: Case Study on a District Level. *Energy Build.* **2016**, *126*, 77–93. [CrossRef]
35. EUR-Lex-32018L0844-EN-EUR-Lex. Available online: https://eur-lex.europa.eu/eli/dir/2018/844/oj (accessed on 15 April 2020).
36. Mulvaney, D. Green New Deal. *Solar Power* **2019**, 47–65. [CrossRef]
37. Australian Building Codes Board. Handbook: Energy Efficiency NCC Volume Two. 2019. Available online: https://www.abcb.gov.au/Resources/Publications/Education-Training/energy-efficiency-ncc-volume-two (accessed on 14 January 2021).
38. International Code Council. *The International Energy Conservation Code (IECC)*. 2000. Available online: https://shop.iccsafe.org/2000-international-energy-conservation-coder-pdf-download.html (accessed on 22 December 2020).
39. HULC Unified Tool LIDER-CALENER, Version 1.0.1493.1049 (Herramienta Unificada LIDER-CALENER, Versión 1.0.1493.1049). Available online: http://www.codigotecnico.org/index.php/menu-recursos/menu-aplicaciones/282-herramienta-unificada-lider-calener (accessed on 1 July 2016).
40. Rakoto-Joseph, O.; Garde, F.; David, M.; Adelard, L.; Randriamanantany, Z. Development of Climatic Zones and Passive Solar Design in Madagascar. *Energy Convers. Manag.* **2009**, *50*, 1004–1010. [CrossRef]
41. Walsh, A.; Cóstola, D.; Labaki, L.C. Review of Methods for Climatic Zoning for Building Energy Efficiency Programs. *Build. Environ.* **2017**, *112*, 337–350. [CrossRef]
42. Ministerio de Fomento Documento Básico HE Ahorro de Energía 2019. *Código Técnico de la Edificacion* **2019**, 1–129.
43. Ferreira, M.; Coelho, M.J.P.; Alves, R.V.L. *Regulamento das Características de Comportamento Térmico de Edifícios (RCCTE): Desenvolvimento de Folha de Cálculo*; Edições Universidade Fernando Pessoa: Porto, Portugal, 2009; pp. 67–75.
44. France. Code de La Construction et de l' Habitation Partie Législative Livre Ier: Dispositions Générales. Titre Préliminaire: Informations Du Parlement En Matière de Logement Partie Législative Livre Ier: Dispositions Générales. *Titre Ier Constr. Des.* **2011**, 2007–2008.
45. Carpio, M.; Jódar, J.; Rodíguez, M.L.; Zamorano, M. A Proposed Method Based on Approximation and Interpolation for Determining Climatic Zones and Its Effect on Energy Demand and CO_2 Emissions from Buildings. *Energy Build.* **2015**, *87*, 253–264. [CrossRef]
46. Lastra-Bravo, X.B.; Fernández-Membrive, V.J.; Flores-Parra, I.; Tolón-Becerra, A. Energy Qualification in Buildings. The Effect of Changes in Construction Methods in the Spanish A4 Climate Zone. *Energy Procedia* **2013**, *42*, 513–522. [CrossRef]
47. Salmerón, J.; Álvarez, S.; Molina, J.; Ruiz, A.; Sánchez, F. Tightening the Energy Consumptions of Buildings Depending on Their Typology and on Climate Severity Indexes. *Energy Build.* **2013**, *58*, 372–377. [CrossRef]
48. State Meteorological Agency-AEMET-Spanish Government. Available online: http://www.aemet.es/es/portada (accessed on 15 April 2021).
49. NOAA ESRL GMD NOAA Solar Calculation. Available online: https://www.esrl.noaa.gov/gmd/grad/solcalc/calcdetails.html (accessed on 20 January 2021).

50. National Platform for Adaptation to Climate Change. Available online: https://www.adaptecca.es/en (accessed on 20 January 2021).

51. Jiang, A.; Zhu, Y.; Elsafty, A.; Tumeo, M. Effects of Global Climate Change on Building Energy Consumption and Its Implications in Florida. *Int. J. Constr. Educ. Res.* **2018**, *14*, 22–45. [CrossRef]

52. Chan, A. Developing Future Hourly Weather Files for Studying the Impact of Climate Change on Building Energy Performance in Hong Kong. *Energy Build.* **2011**, *43*, 2860–2868. [CrossRef]

53. Burden, R.L.; Faires, J.D.; Burden, A.M. *Numerical Analysis*; Cengage: New York, NY, USA, 2016; ISBN 9781305253667.

54. Buhmann, M.D. Radial basis functions. *Acta Numer.* **2000**, *9*, 1–38. [CrossRef]

55. López-Ochoa, L.M.; Las-Heras-Casas, J.; López-González, L.M.; García-Lozano, C. Environmental and Energy Impact of the Epbd in Residential Buildings in Cold Mediterranean Zones: The Case of Spain. *Energy Build.* **2017**, *150*, 567–582. [CrossRef]

56. Royal Decree 314/2006 of March 17, Approving the Technical Building Code (Real Decreto 314/2006, de 17 de Marzo, Por El Que Se Aprueba El Código Técnico de La Edificación). Available online: http://www.boe.es/boe/dias/2006/03/28/pdfs/A11816-11831.pdf (accessed on 20 July 2020).

57. Avendaño-Vera, C.; Martinez-Soto, A.; Marincioni, V. Determination of Optimal Thermal Inertia of Building Materials for Housing in Different Chilean Climate Zones. *Renew. Sustain. Energy Rev.* **2020**, *131*, 110031. [CrossRef]

58. Parker, J. The Leeds Urban Heat Island and Its Implications for Energy Use and Thermal Comfort. *Energy Build.* **2021**, *235*, 110636. [CrossRef]

59. Adloff, F.; Somot, S.; Sevault, F.; Jordà, G.; Aznar, R.; Déqué, M.; Herrmann, M.; Marcos, M.; Dubois, C.; Padorno, E.; et al. Mediterranean Sea Response to Climate Change in an Ensemble of Twenty First Century Scenarios. *Clim. Dyn.* **2015**, *45*, 2775–2802. [CrossRef]